Turing Instability Analysis of A Memristive Cellular Neural Networks

Xinhui Wang, *Member, IAENG, Zunxian Li, Member, IAENG, and Liangbo Sun, Member, IAENG*

***Abstract*—By using the concepts of Kronecker sum and Kronecker product, the matrix form of decoupling method is proposed to analyze the Turing instability of the equilibria for a memristive cellular neural networks under the zero-flux boundary conditions. It is shown that Turing instability can never occur at the zero equilibrium nor at the non-zero equilibrium for the self-diffusion case, while Turing instability may occur at the non-zero equilibrium for the cross-diffusion case. Furthermore, the local stability of the non-zero equilibrium determined by system parameters is studied. Finally, several numerical simulations are given. This matrix form of decoupling method can be extended to study memristive cellular neural networks with other boundary conditions.**

***Index Terms*—cellular neural networks, Turing instability, self-diffusion, cross-diffusion.**

I. Introduction

CELLULAR neural networks (abbreviated as CNNs) are arrays of some locally interconnected simple processors. Since CNNs were proposed by Chua and Yang in [2], this model has achieved significant developments in both theories and applications. In applications, CNNs have been widely used in practical problems, such as image processing, pattern recognition, and solving differential equations due to their simplicity and high computational efficiency. Theoretically, the dynamics of CNNs are complex since this model can be viewed as coupled ordinary differential equations. These dynamics include Turing instability, Turing patterns, Hopf bifurcation and chaos. We refer to the references [1]-[6] for more details, wherein the concept of Turing instability was proposed in Turing's famous paper [1]. Turing instability is also called "diffusion-driven instability".

As a special kind of CNNs, memristive cellular neural networks (abbreviated as MCNNs) incorporate memristors, which are usually non-linear resistive components. The introduction of memristors enhances the functionality and adaptability of CNNs, allowing them to generate complicated patterns and provide a novel paradigm for the design of advanced computational systems. From a mathematical perspective, MCNNs can be conceptualized as reaction-diffusion equations, characterized by a two-dimensional array of interconnected cells that consist of two essential components, i.e., a linear passive capacitor and a nonlinear active memristor. We refer to the references [7]-[9] for more details.

Manuscript received December 16, 2024; revised June 24, 2025. This work was supported in part by Natural Science Foundation of China under Grant 11601384 and Tianjin Municipal Education Commission Research Project under Grant 2018KJ147.

X.H. Wang is a postgraduate student in the Department of Mathematics, Tianjin University of Technology, Tianjin, 300384, China. (e-mail:1373692951@qq.com).

Z.X. Li is an associate professor in the Department of Mathematics, Tianjin University of Technology, Tianjin, 300384, China. (corresponding author, e-mail:lizunxian_hs@163.com).

L.B. Sun is a postgraduate student in the Department of Mathematics, Tianjin University of Technology, Tianjin, 300384, China. (e-mail:2261511004@qq.com).

Fig. 1: Basic cell

As shown in reference [7], a detailed description of a cell with a memristor was illustrated in Fig. 1.

The cell consists of two components in parallel: a linear passive capacitor C and a memristor M. By applying the Kirchhoff laws, the dynamical equations of the cell are

$$C\dot{v} = -\beta(\phi^2 - 1)v,$$
$$\dot{\phi} = v - \alpha\phi - v\phi,$$

where v represents the voltage of the capacitor, ϕ denotes the internal state function of the memristor with the memristance function $R = \beta(\phi^2 - 1)$ and α, β are constant parameters. In the following, we always assume

$$(H1) : \alpha > 0, \beta > 0,$$

the same as in [8].

Let $x = v$, $y = \phi$ and $\gamma = \frac{1}{C}$, then the above dynamical equations become

$$\begin{cases} \dot{x} = -\gamma\beta(y^2 - 1)x, \\ \dot{y} = x - \alpha y - yx. \end{cases} \tag{1}$$

Based on Eq.(1), the dynamical equations of the $M \times N$ MCNNs are further established in [8]. The equations are

$$\begin{cases} \dot{x}_{i,j} = -\gamma\beta(y_{i,j}^2 - 1)x_{i,j} \\ +D_{11}(x_{i-1,j} + x_{i+1,j} + x_{i,j-1} + x_{i,j+1} - 4x_{i,j}) \\ +D_{12}(y_{i-1,j} + y_{i+1,j} + y_{i,j-1} + y_{i,j+1} - 4y_{i,j}), \\ \dot{y}_{i,j} = x_{i,j} - \alpha y_{i,j} - x_{i,j}y_{i,j} \\ +D_{21}(x_{i-1,j} + x_{i+1,j} + x_{i,j-1} + x_{i,j+1} - 4x_{i,j}) \\ +D_{22}(y_{i-1,j} + y_{i+1,j} + y_{i,j-1} + y_{i,j+1} - 4y_{i,j}), \end{cases} \tag{2}$$

where $x_{i,j}$ and $y_{i,j}$ with $i \in \{0, 1, 2, \cdots, M-1\}$ and $j \in \{0, 1, 2, \cdots, N-1\}$ represent the voltages of the capacitor and the state functions of the cell in the i-row and j-column, respectively. D_{11} and D_{22} denote the self-diffusion coefficients, while D_{12} and D_{21} denote the cross-diffusion coefficients, respectively. To ensure diffusion coupling is dissipative as in [8], we further assume

$$(H2) : det(D) = D_{11}D_{22} - D_{12}D_{21} > 0.$$

By introducing the following notations

$$\begin{cases} \nabla^2 x_{i,j} = x_{i-1,j} + x_{i+1,j} + x_{i,j-1} + x_{i,j+1} - 4x_{i,j}, \\ \nabla^2 y_{i,j} = y_{i-1,j} + y_{i+1,j} + y_{i,j-1} + y_{i,j+1} - 4y_{i,j}, \end{cases} \tag{3}$$

Eq.(2) can be rewritten as

$$\begin{cases} \dot{x}_{i,j} = f(x_{i,j}, y_{i,j}) + D_{11}\nabla^2 x_{i,j} + D_{12}\nabla^2 y_{i,j}, \\ \dot{y}_{i,j} = g(x_{i,j}, y_{i,j}) + D_{21}\nabla^2 x_{i,j} + D_{22}\nabla^2 y_{i,j}, \end{cases} \tag{4}$$

where $f(x, y) = -\gamma\beta(y^2 - 1)x, g(x, y) = x - \alpha y - xy$.

We further consider the zero-flux boundary conditions

$$\begin{aligned} &x_{-1,j}(t) = x_{0,j}(t), x_{M,j}(t) = x_{M-1,j}(t), \\ &x_{i,-1}(t) = x_{i,0}(t), x_{i,N}(t) = x_{i,N-1}(t), \\ &y_{-1,j}(t) = y_{0,j}(t), y_{M,j}(t) = y_{M-1,j}(t), \\ &y_{i,-1}(t) = y_{i,0}(t), y_{i,N}(t) = y_{i,N-1}(t). \end{aligned} \tag{5}$$

The boundary conditions (5) correspond to the case when the free ends of all coupling (grid) resistors are not connected as illustrated in the reference [5].

Eq.(4) under the boundary conditions (5) has two constant equilibria, i.e., the zero equilibrium

$$E_0 = (0, 0, 0, 0, \cdots, 0, 0) \in R^{M\times N}$$

and non-zero equilibrium

$$E_1 = (-\frac{\alpha}{2}, -1, -\frac{\alpha}{2}, -1, \cdots, -\frac{\alpha}{2}, -1) \in R^{M\times N}.$$

In this paper, we introduce the matrix form of the decoupling method by using Kronecker sum and Kronecker product. There are many applications of Kronecker sum and Kronecker product. For example, they were used to study linear error block codes in [10]. Here we use these concepts to prove the matrix form of the decoupling method and further to study the Turing instability of E_0 and E_1. To be precise, in Section II, we show that Turing instability can never occur at E_0. Furthermore, we study the stability of E_1 by using the matrix form of the decoupling method. Then we show that Turing instability can never occur at E_1 for the self-diffusion case, while it may occur at E_1 for the cross-diffusion case. In Section III, we give some numerical simulations to show the derived theoretical results in Section II. Finally, we give some conclusions and discussions.

II. Turing instability analysis

Without loss of generality, we let $\gamma = 1$ and we have

Proposition 1. *The equilibrium $(0, 0)$ of Eq.(1) is unstable, while the equilibrium $(-\frac{\alpha}{2}, -1)$ of Eq.(1) is locally asymptotically stable.*

Proof: The Jacobi matrix of Eq.(1) at $(0, 0)$ is

$$J_0 = \begin{pmatrix} \beta & 0 \\ 1 & -\alpha \end{pmatrix}, \tag{6}$$

hence the corresponding characteristic equation is

$$\lambda^2 - T_0\lambda + D_0 = 0, \tag{7}$$

where $T_0 = \beta - \alpha$, $D_0 = -\alpha\beta$. By $(H1)$, we have $D_0 < 0$, which suggests that one of roots of the characteristic equation Eq.(7) is positive. Hence $(0, 0)$ is unstable.

Meanwhile, the Jacobi matrix of Eq.(1) at $(-\frac{\alpha}{2}, -1)$ is

$$J_0 = \begin{pmatrix} 0 & -\alpha\beta \\ 2 & -\frac{\alpha}{2} \end{pmatrix}, \tag{8}$$

hence the corresponding characteristic equation is

$$\lambda^2 - T_1\lambda + D_1 = 0, \tag{9}$$

where $T_1 = -\frac{\alpha}{2}$, $D_1 = 2\alpha\beta$. By $(H1)$, we have $T_1 < 0$ and $D_1 > 0$, which suggests that the real parts of both roots of the characteristic equation Eq.(9) are negative. Hence the equilibrium $(-\frac{\alpha}{2}, -1)$ is locally asymptotically stable. ■

By Proposition 1, it is seen that Turing instability can never occur at E_0. Hence for the rest of this section, we mainly focus on the local stability of E_1.

The linearized equations of Eq.(4) located at E_1 are

$$\begin{cases} \dot{x}_{i,j} = -\alpha\beta x_{i,j} + D_{11}\nabla^2 x_{i,j} + D_{12}\nabla^2 y_{i,j}, \\ \dot{y}_{i,j} = 2x_{i,j} - \dfrac{\alpha}{2} y_{i,j} + D_{21}\nabla^2 x_{i,j} + D_{22}\nabla^2 y_{i,j}. \end{cases} \tag{10}$$

Then we introduce the matrix form of decoupling method. For this purpose, we denote

$$\begin{aligned} X = (&x_{0,0}, y_{0,0}, x_{0,1}, y_{0,1}, \cdots, x_{0,N-1}, y_{0,N-1}, \\ &x_{1,0}, y_{1,0}, x_{1,1}, y_{1,1}, \cdots, x_{1,N-1}, y_{1,N-1}, \\ &\cdots\ \cdots\ \cdots, \\ &x_{M-1,0}, y_{M-1,0}, x_{M-1,1}, y_{M-1,1}, \\ &\cdots, x_{M-1,N-1}, y_{M-1,N-1})^T, \end{aligned} \tag{11}$$

Then Eq.(10) can be rewritten as the matrix form

$$\dot{X} = LX, \tag{12}$$

Under the boundary conditions (5), it is seen that

$$L = (\Delta_M \oplus \Delta_N) \otimes D + I_{MN} \otimes F,$$

according to the reference [11]. Herein

$$D = \begin{pmatrix} D_{11} & D_{12} \\ D_{21} & D_{22} \end{pmatrix}, \mathrm{F} = \begin{pmatrix} 0 & -\alpha\beta \\ 2 & -\frac{\alpha}{2} \end{pmatrix},$$

$$\Delta_M = \begin{pmatrix} -1 & 1 & 0 & 0 & \cdots & 0 & 0 & 0 \\ 1 & -2 & 1 & 0 & \cdots & 0 & 0 & 0 \\ 0 & 1 & -2 & 1 & \cdots & 0 & 0 & 0 \\ \vdots & \vdots & \vdots & \vdots & \ddots & \vdots & \vdots & \vdots \\ 0 & 0 & 0 & 0 & \cdots & 1 & -2 & 1 \\ 0 & 0 & 0 & 0 & \cdots & 0 & 1 & -1 \end{pmatrix}_{M\times M},$$

$$\Delta_N = \begin{pmatrix} -1 & 1 & 0 & 0 & \cdots & 0 & 0 & 0 \\ 1 & -2 & 1 & 0 & \cdots & 0 & 0 & 0 \\ 0 & 1 & -2 & 1 & \cdots & 0 & 0 & 0 \\ \vdots & \vdots & \vdots & \vdots & \ddots & \vdots & \vdots & \vdots \\ 0 & 0 & 0 & 0 & \cdots & 1 & -2 & 1 \\ 0 & 0 & 0 & 0 & \cdots & 0 & 1 & -1 \end{pmatrix}_{N\times N},$$

and the notations $\oplus$ and $\otimes$ denote Kronecker sum and Kronecker product, respectively, while I_{MN} represents the MN-order identity matrix. Then we have

Theorem 1. *Matrix L is similar to the following block diagonal matrix*

$$L_d = \begin{pmatrix} L_{0,0} & & & & & & & & \\ & L_{0,1} & & & & & & & \\ & & \ddots & & & & & & \\ & & & L_{0,N-1} & & & & & \\ & & & & L_{1,0} & & & & \\ & & & & & L_{1,1} & & & \\ & & & & & & \ddots & & \\ & & & & & & & L_{1,N-1} & \\ & & & & & & & & \ddots \\ & & & & & & & & & L_{M-1,N-1} \end{pmatrix},$$

where

$$L_{m,n} = \begin{pmatrix} -D_{11}k_{mn}^2 & -D_{12}k_{mn}^2 - \alpha\beta \\ -D_{21}k_{mn}^2 + 2 & -D_{22}k_{mn}^2 - \frac{\alpha}{2} \end{pmatrix}$$

and

$$-k_{mn}^2 = -k_m^2 - k_n^2 = -4(sin^2\frac{m\pi}{2M} + sin^2\frac{n\pi}{2N})$$

with $m \in \{0, 1, 2, \cdots, M-1\}$ *and* $n \in \{0, 1, 2, \cdots, N-1\}$.

Proof:

Define the matrices

$$\Phi_N = \begin{pmatrix} \phi_N(0,0) & \phi_N(0,1) & \phi_N(0,2) & \dots & \phi_N(0,N-1) \\ \phi_N(1,0) & \phi_N(1,1) & \phi_N(1,2) & \dots & \phi_N(1,N-1) \\ \phi_N(2,0) & \phi_N(2,1) & \phi_N(2,2) & \dots & \phi_N(2,N-1) \\ \vdots & \vdots & \vdots & \ddots & \vdots \\ \phi_N(N-1,0) & \phi_N(N-1,1) & \phi_N(N-1,2) & \dots & \phi_N(N-1,N-1) \end{pmatrix},$$

and

$$\Phi_M = \begin{pmatrix} \phi_M(0,0) & \phi_M(0,1) & \phi_M(0,2) & \dots & \phi_M(0,M-1) \\ \phi_M(1,0) & \phi_M(1,1) & \phi_M(1,2) & \dots & \phi_M(1,M-1) \\ \phi_M(2,0) & \phi_M(2,1) & \phi_M(2,2) & \dots & \phi_M(2,M-1) \\ \vdots & \vdots & \vdots & \ddots & \vdots \\ \phi_M(M-1,0) & \phi_M(M-1,1) & \phi_M(M-1,2) & \dots & \phi_M(M-1,M-1) \end{pmatrix},$$

where

$$\phi_N(m,n) = \cos\frac{(2n+1)m\pi}{2N}, \phi_M(m,n) = \cos\frac{(2n+1)m\pi}{2M}.$$

Denote $\phi(m,n)$ as either $\phi_N(m,n)$ or $\phi_M(m,n)$. According to [12], we have

$$\phi(m, n-1) + \phi(m, n+1) - 2\phi(m,n) = -k_m^2\phi(m,n),$$

and the following orthogonal conditions

$$\langle\phi(m_1,n), \phi(m_2,n)\rangle \begin{cases} = 0, m_1 \neq m_2, \\ \neq 0, m_1 = m_2, \end{cases} \tag{13}$$

where $m_1, m_2 \in \{0, 1, 2, \cdots, M-1\}$. Let

$$\Phi = \Phi_M \otimes \Phi_N \otimes I_2. \tag{14}$$

Then

$$\Phi^{-1} = \Phi_M^{-1} \otimes \Phi_N^{-1} \otimes I_2,$$

where V^{-1} denotes the inverse matrix of the matrix V and I_2 denotes the 2×2-order identity matrix.

Then we have

$$\begin{aligned} &\Phi L\Phi^{-1} = (\Phi_M \otimes \Phi_N \otimes I_2)((\Delta_M \oplus \Delta_N) \otimes D \\ &+I_{MN} \otimes F)(\Phi_M^{-1} \otimes \Phi_N^{-1} \otimes I_2) \\ &= (\Phi_M \otimes \Phi_N \otimes I_2)((\Delta_M \oplus \Delta_N) \otimes D)(\Phi_M^{-1} \otimes \Phi_N^{-1} \otimes I_2) \\ &+(\Phi_M \otimes \Phi_N \otimes I_2)(I_{MN} \otimes F)(\Phi_M^{-1} \otimes \Phi_N^{-1} \otimes I_2). \end{aligned} \tag{15}$$

For the first part of the sums in (15), we have

$$\begin{aligned} &(\Phi_M \otimes \Phi_N \otimes I_2)((\Delta_M \oplus \Delta_N) \otimes D)(\Phi_M^{-1} \otimes \Phi_N^{-1} \otimes I_2) \\ &= (\Phi_M \otimes \Phi_N)((\Delta_M \oplus \Delta_N))(\Phi_M^{-1} \otimes \Phi_N^{-1}) \otimes D \\ &= \big[(\Phi_M \otimes \Phi_N)(\Delta_M \otimes I_N)(\Phi_M^{-1} \otimes \Phi_N^{-1}) + \\ &(\Phi_M \otimes \Phi_N)(I_M \otimes \Delta_N)(\Phi_M^{-1} \otimes \Phi_N^{-1})\big] \otimes D \\ &= \big[(\Phi_M\Delta_M\Phi_M^{-1}) \otimes (\Phi_N I_N \Phi_N^{-1}) + \\ &(\Phi_M I_M \Phi_M^{-1}) \otimes (\Phi_N\Delta_N\Phi_N^{-1})\big] \otimes D \\ &= \big[(\Phi_M\Delta_M\Phi_M^{-1}) \otimes I_N + I_M \otimes (\Phi_N\Delta_N\Phi_N^{-1})\big] \otimes D \\ &= [\Delta_{Md} \oplus \Delta_{Nd}] \otimes D, \end{aligned}$$

where

$$\Delta_{Md} = \Phi_M\Delta_M\Phi_M^{-1} = \begin{pmatrix} -k_0^2 & & & \\ & -k_1^2 & & \\ & & \ddots & \\ & & & -k_{M-1}^2 \end{pmatrix},$$

and

$$\Delta_{Nd} = \Phi_N\Delta_N\Phi_N^{-1} = \begin{pmatrix} -k_0^2 & & & \\ & -k_1^2 & & \\ & & \ddots & \\ & & & -k_{N-1}^2 \end{pmatrix}.$$

For the second part of the sums in (15), we have

$$\begin{aligned} &(\Phi_M \otimes \Phi_N \otimes I_2)(I_{MN} \otimes F)(\Phi_M^{-1} \otimes \Phi_N^{-1} \otimes I_2) \\ &= (\Phi_M \otimes \Phi_N)I_{MN}(\Phi_M^{-1} \otimes \Phi_N^{-1}) \otimes F \\ &= I_{MN} \otimes F. \end{aligned}$$

Hence we have

$$\Phi L\Phi^{-1} = [\Delta_{Md} \oplus \Delta_{Nd}] \otimes D + I_{MN} \otimes F = L_d.$$

■

We define the following linear transformation

$$X = \Phi^{-1}Y, \tag{16}$$

where

$$\begin{aligned} Y = (&\hat{x}_{0,0}, \hat{y}_{0,0}, \hat{x}_{0,1}, \hat{y}_{0,1}, \cdots, \hat{x}_{0,N-1}, \hat{y}_{0,N-1}, \\ &\hat{x}_{1,0}, \hat{y}_{1,0}, \hat{x}_{1,1}, \hat{y}_{1,1}, \cdots, \hat{x}_{1,N-1}, \hat{y}_{1,N-1}, \\ &\cdots\ \cdots\ \cdots, \\ &\hat{x}_{M-1,0}, \hat{y}_{M-1,0}, \hat{x}_{M-1,1}, \hat{y}_{M-1,1}, \cdots, \\ &\hat{x}_{M-1,N-1}, \hat{y}_{M-1,N-1})^T. \end{aligned} \tag{17}$$

By Theorem 1 and the transformation (16), Eq.(12) becomes

$$\dot{Y} = \Phi\dot{X} = \Phi L\Phi^{-1}Y = L_dY. \tag{18}$$

Hence the local stability of E_1 depends on the eigenvalues of matrix L_d. The eigenvalues of L_d are the roots of the following quadratic equation with one unknown

$$\lambda^2 - T_{mn}\lambda + D_{mn} = 0, \tag{19}$$

where $m, n \in \{0, 1, 2, \cdots, (M-1)(N-1)\}$ and

$$\begin{cases} T_{mn} &= -(D_{11} + D_{22})k_{mn}^2 - \frac{\alpha}{2}, \\ D_{mn} &= (D_{11}D_{22} - D_{12}D_{21})k_{mn}^4 + \\ & (\frac{\alpha}{2}D_{11} + 2D_{12} - \alpha\beta D_{21})k_{mn}^2 + 2\alpha\beta. \end{cases} \tag{20}$$

By $(H1)$, we have $T_{mn} < 0$ while the signs of D_{mn} are uncertain. By $(H2)$, we further have $D_{mn} > 0$ when $\frac{\alpha}{2}D_{11} + 2D_{12} - \alpha\beta D_{21} \geq 0$. Then all of the roots of Eq.(19) have negative real parts. Hence we have

Theorem 2. *Assuming* $\frac{\alpha}{2}D_{11} + 2D_{12} - \alpha\beta D_{21} \geq 0$*, the equilibrium* E_1 *is locally asymptotically stable.*

If $\frac{\alpha}{2}D_{11} + 2D_{12} - \alpha\beta D_{21} < 0$, then the analysis on the eigenvalues of L_d becomes complicated. For this, define

$$\begin{aligned} J(\xi) =&(D_{11}D_{22} - D_{12}D_{21})\xi^2 + \\ &(\frac{\alpha}{2}D_{11} + 2D_{12} - \alpha\beta D_{21})\xi + 2\alpha\beta, \xi \geq 0. \end{aligned}$$

Then it is seen that $J(k_{mn}^2) = D_{mn}$ and the discriminant of $J(\xi) = 0$ is

$$\begin{aligned} \Delta_1 =&(\frac{1}{2}D_{11} - \beta D_{21})^2\alpha^2 + \\ &(D_{11}D_{12} + 2\beta D_{12}D_{21} - 4\beta D_{11}D_{22})2\alpha + 4D_{12}^2. \end{aligned}$$

Hence $J(\xi) = 0$ has a unique root

$$\xi_0 = \frac{2\alpha\beta D_{21} - 4D_{12} - \alpha D_{11}}{4(D_{11}D_{22} - D_{12}D_{21})},$$

if $\Delta_1 = 0$, while $J(\xi) = 0$ has two roots

$$\xi_{1,2} = \frac{2\alpha\beta D_{21} - 4D_{12} - \alpha D_{11} \mp 2\sqrt{\Delta_1}}{4(D_{11}D_{22} - D_{12}D_{21})},$$

if $\Delta_1 > 0$.

It is seen further that Δ_1 is a quadratic function of α, which can be denoted by the following quadratic function

$$\begin{aligned} K(z) =&(\frac{1}{2}D_{11} - \beta D_{21})^2 z^2 + \\ &(2D_{11}D_{12} + 4\beta D_{12}D_{21} - 8\beta D_{11}D_{22})z + 4D_{12}^2. \end{aligned}$$

The discriminant of $K(z) = 0$ is

$$\Delta_2 = 32\beta D_{11}(D_{11}D_{22} - D_{12}D_{21})(2\beta D_{22} - D_{12}).$$

It is easy to see that

(i) $\Delta_2 > 0$ if $\frac{D_{12}}{D_{22}} < 2\beta$;

(ii) $\Delta_2 = 0$ if $\frac{D_{12}}{D_{22}} = 2\beta$; and

(iii) $\Delta_2 < 0$ if $\frac{D_{12}}{D_{22}} > 2\beta$.

We note that the case (iii) contradicts the conditions $(H1)$ and $(H2)$. In fact, we have

Lemma 1. *If $\frac{\alpha}{2}D_{11} + 2D_{12} - \alpha\beta D_{21} < 0$, then $\frac{D_{12}}{D_{22}} \le 2\beta$.*

Proof: By contradiction, we assume $\frac{D_{12}}{D_{22}} > 2\beta$. Then by the inequality $\frac{\alpha}{2}D_{11} + 2D_{12} - \alpha\beta D_{21} < 0$, we have $2\beta > \frac{D_{11}}{D_{21}} + \frac{4}{\alpha}\frac{D_{12}}{D_{21}}$. By $(H2)$, we have $\frac{D_{11}}{D_{21}} > \frac{D_{12}}{D_{22}}$. Hence $\frac{D_{12}}{D_{22}} > 2\beta > \frac{D_{11}}{D_{21}} + \frac{4}{\alpha}\frac{D_{12}}{D_{21}} > \frac{D_{12}}{D_{21}} + \frac{4}{\alpha}\frac{D_{12}}{D_{21}}$. It is a contradiction. ■

Hence we only need to consider the cases (i) and (ii). For both cases, $K(z) = 0$ has two roots, which are multiple when $\frac{D_{12}}{D_{22}} = 2\beta$. In the following, we denote the two roots of $K(z) = 0$ to be

$$z_{1,2} = \frac{4\beta D_{11}D_{22} - 2\beta D_{12}D_{21} - D_{11}D_{12} \mp \frac{1}{2}\sqrt{\Delta_2}}{(\frac{1}{2}D_{11} - \beta D_{21})^2}.$$

Then we have the following three lemmas.

Lemma 2. *Assuming $\frac{D_{12}}{D_{22}} \le 2\beta, \alpha \in (z_1, z_2)$, E_1 is locally asymptotically stable.*

Lemma 3. *Assuming $\frac{D_{12}}{D_{22}} \le 2\beta, \alpha = z_1$ or z_2,*

1) *E_1 is locally asymptotically stable when $k_{mn}^2 \neq \xi_0, \forall m, n$; or*
2) *E_1 is the critical case when there exist m^*, n^* such that $k_{m^*n^*}^2 = \xi_0$.*

Lemma 4. *Assuming $\frac{D_{12}}{D_{22}} \le 2\beta, \alpha \notin [z_1, z_2]$,*

1) *E_1 is locally asymptotically stable when $k_{mn}^2 \notin [\xi_1, \xi_2], \forall m$; or*
2) *E_1 is unstable when there exist m^*, n^* such that $k_{m^*n^*}^2 \in (\xi_1, \xi_2)$; or*
3) *E_1 is the critical case when there exist m^*, n^* such that $k_{m^*n^*}^2 = \xi_1$ or ξ_2.*

Based on the above lemmas, we derive

Theorem 3. *Assuming $\frac{\alpha}{2}D_{11} + 2D_{12} - \alpha\beta D_{21} < 0$, the stability of E_1 can be determined by the following Table I, where the symbol "L.A.S." represents E_1 is locally asymptotically stable.*

By Theorems 2 and 3, it is seen that Turing instability can never occur at E_1 for the self-diffusion case, i.e., $D_{12} = D_{21} = 0$, while Turing instability may occur at E_1 for the cross-diffusion case, i.e., $D_{12} \neq 0$ or $D_{21} \neq 0$.

III. Numerical simulations

In this section, we present several numerical simulations using MATLAB to illustrate the theoretical results from Theorems 2 and 3. To this end, we define eight groups of system parameters and analyze the stability of E_1 based on the framework in Section II. To be precise, the stability results for Groups 1-2 (Table II) are derived from Theorem 2, while those for Groups 3-8 (Table III) are derived from Theorem 3.

Based on these system parameters in Tables II and III, the following figures, i.e., Fig.2-Fig.9, present the numerical simulations, wherein interpolation is used in order to get better visual effects. In each figure, the first row displays the distribution of $x_{i,j}$, while the second row shows the distribution of $y_{i,j}$. To be precise, the first one in each row shows the distribution at inital time, the second one in each row shows the distribution at the final time, and the third one in each row shows the thermodynamic distribution at the final time. In addition, we choose randomized initial conditions for all numerical simulations.

From these figures, it can be observed that the results on the stability of E_1 coincide with the theoretical analyses. That is, for the system parameters in Groups 1-5, E_1 is locally asymptotically stable, while for the system parameters in Groups 6-8 , E_1 is unstable. Moreover, for those parameters in Groups 6-8, different Turing patterns arise. In fact, strip patterns are obtained for Group 6, mixed states of strip and spot patterns are obtained for Group 7 and spot patterns are obtained for Group 8. We refer to [13] for more details.

IV. Conclusions and discussions

In this paper, we develop the matrix form of the decoupling method to study the Turing instability of MCNNs under zero-flux boundary conditions. However, more should be considered.

1. The zero-flux boundary conditions are assumed in the present paper. However, there are other kinds of boundary conditions. For example, the periodic boundary conditions are discussed in [12]. We suggest that this method should also be valid for these boundary conditions.

2. Turing patterns are presented through numerical simulations in the present paper, without theoretical analysis. We suggest that these Turing patterns might be caused by other dynamical behaviors, such as steady-state bifurcation, Hopf bifurcation, traveling waves and spiral waves. We refer to [13], [14] for examples. We will consider the theoretical analysis of these Turing patterns and their relation to other dynamical behaviors in the future.

References

[1] A. M. Turing, "The chemical basis of morphogenesis," Philosophical Transactions of the Royal Society of London. Series B, vol.237, pp.37-72, 1952.

[2] L. O. Chua and L. Yang, "Cellular neural networks: theory," IEEE Transactions on Circuits and Systems, vol.35, no.10, pp.1257-1272, 1988.

[3] L. O. Chua and L. Yang, "Cellular neural networks: applications," IEEE Transactions on Circuits and Systems, vol.35, no.10, pp.1273-1290, 1988.

[4] Z. X. Li and C. Y. Xia, "Turing Instability and Hopf Bifurcation in Cellular Neural Networks," International Journal of Bifurcation and Chaos, vol.31, no.08, pp.2150143:1-17, 2021.

TABLE I: Stability of E_1

Stability	Range of parameters
L.A.S.	$\frac{D_{12}}{D_{22}} \leq 2\beta$ and $\alpha \in (z_1, z_2)$; or $\frac{D_{12}}{D_{22}} \leq 2\beta$ and $\alpha = z_1$ or z_2 and $k_{mn}^2 \neq \xi_0, \forall m, n$; or $\frac{D_{12}}{D_{22}} \leq 2\beta$ and $\alpha \notin [z_1, z_2]$ and $k_{mn}^2 \notin [\xi_1, \xi_2], \forall m, n$.
unstable	$\frac{D_{12}}{D_{22}} \leq 2\beta$ and $\alpha \notin [z_1, z_2]$ and exist m^*, n^* such that $k_{m^*n^*}^2 \in (\xi_1, \xi_2)$.
critical case	$\frac{D_{12}}{D_{22}} \leq 2\beta$ and $\alpha = z_1$ or z_2 and exist m^*, n^*such that $k_{m^*n^*}^2 = \xi_0$; or $\frac{D_{12}}{D_{22}} \leq 2\beta$ and $\alpha \notin [z_1, z_2]$ and exist m^*, n^* such that $k_{m^*n^*}^2 = \xi_1$ or ξ_2.

TABLE II: System parameters and stability results for E_1 based on Theorem 2.

Group	Parameters	Discriminant Conditions	Results
1	$D_{11} = 4, D_{12} = 1, D_{21} = 6, D_{22} = 4,$ $M = N = 30,$ $\alpha = 3, \beta = 0.2.$	$\alpha > 0, \beta > 0,$ and $\frac{\alpha}{2}D_{11} + 2D_{12} - \alpha\beta D_{21} \geq 0.$	L.A.S.
2	$D_{11} = 6, D_{12} = 0, D_{21} = 0, D_{22} = 5,$ $M = N = 30,$ $\alpha = 0.6, \beta = 1.5.$	$\alpha > 0, \beta > 0,$ and $\frac{\alpha}{2}D_{11} + 2D_{12} - \alpha\beta D_{21} \geq 0.$	L.A.S.

TABLE III: System parameters and stability results for E_1 based on Theorem 3.

Group	Parameters	Discriminant Conditions	Results
3	$D_{11} = 4, D_{12} = 1, D_{21} = 6, D_{22} = 4,$ $M = N = 50, \alpha = 1, \beta = 1.5,$ $z_1 = 0.0272, z_2 = 2.993.$	$\alpha > 0, \frac{D_{12}}{D_{22}} \leq 2\beta,$ $\alpha \in (z_1, z_2),$ and $\frac{\alpha}{2}D_{11} + 2D_{12} - \alpha\beta D_{21} < 0.$	L.A.S.
4	$D_{11} = 4, D_{12} = 1, D_{21} = 6, D_{22} = 4,$ $M = N = 5, \alpha = 2.9931, \beta = 1.5,$ $z_1 = 0.0273, z_2 = 2.9931, \xi_0 = 0.9475,$ $k_{mn}^2 = 0, 0.0979, 0.3820, 0.7639, 1.3850, ..., 7.2361.$	$\alpha > 0, \frac{D_{12}}{D_{22}} \leq 2\beta,$ $\alpha = z_2,$ $k_{mn}^2 \neq \xi_0, \forall m, n.$ and $\frac{\alpha}{2}D_{11} + 2D_{12} - \alpha\beta D_{21} < 0.$	L.A.S.
5	$D_{11} = 4, D_{12} = 1, D_{21} = 6, D_{22} = 4,$ $M = N = 5, \alpha = 3, \beta = 1.5,$ $z_1 = 0.0272, z_2 = 2.993,$ $\xi_1 = 0.9000, \xi_2 = 1.000,$ $k_{mn}^2 = 0, 0.0979, 0.3820, 0.7639, 1.3850, ..., 7.2361.$	$\alpha > 0, \frac{D_{12}}{D_{22}} \leq 2\beta,$ $\alpha \notin [z_1, z_2],$ $k_{mn}^2 \notin [\xi_1, \xi_2], \forall m, n,$ and $\frac{\alpha}{2}D_{11} + 2D_{12} - \alpha\beta D_{21} < 0.$	L.A.S.
6	$D_{11} = 4, D_{12} = 1, D_{21} = 6, D_{22} = 4,$ $M = N = 50, \alpha = 5, \beta = 1.5,$ $\xi_1 = 0.5433, \xi_2 = 2.7557.$	$\alpha > 0, \frac{D_{12}}{D_{22}} \leq 2\beta,$ $\alpha \notin [z_1, z_2]$, $k_{10,10}^2 = 0.6227 \in (\xi_1, \xi_2),$ and $\frac{\alpha}{2}D_{11} + 2D_{12} - \alpha\beta D_{21} < 0.$	unstable
7	$D_{11} = 4, D_{12} = 1, D_{21} = 6, D_{22} = 4,$ $M = N = 50, \alpha = 4, \beta = 1.5,$ $\xi_1 = 0.6, \xi_2 = 2.$	$\alpha > 0, \frac{D_{12}}{D_{22}} \leq 2\beta,$ $\alpha \notin [z_1, z_2]$, $k_{10,10}^2 = 0.6227 \in (\xi_1, \xi_2),$ and $\frac{\alpha}{2}D_{11} + 2D_{12} - \alpha\beta D_{21} < 0.$	unstable
8	$D_{11} = 4, D_{12} = 1, D_{21} = 6, D_{22} = 4,$ $M = N = 50, \alpha = 3, \beta = 1.5,$ $\xi_1 = 0.6, \xi_2 = 2.$	$\alpha > 0, \frac{D_{12}}{D_{22}} \leq 2\beta,$ $\alpha \notin [z_1, z_2]$, $k_{10,10}^2 = 0.6227 \in (\xi_1, \xi_2),$ and $\frac{\alpha}{2}D_{11} + 2D_{12} - \alpha\beta D_{21} < 0.$	unstable

[5] L. Goras, L. O. Chua and D. M. W. Leenaerts, "Turing patterns in CNNs. I. Once over lightly," IEEE Transactions on Circuits and Systems I: Fundamental Theory and Applications, vol.42, no.10, pp.602-611, 1995.

[6] C. J. Xu, and P. L. Li, "Matrix measure strategies for stability of cellular neural networks with proportional delays," IAENG International Journal of Applied Mathematics, vol.46, no.3, pp.305-310, 2016.

[7] B. Muthuswamy and L. O. Chua, "Simplest Chaotic Circuit," Int. J. Bifurc. Chaos, vol.20, no.05, pp.1567-1580, 2010.

[8] M. Bucolo, A. Buscarino, C. Corradino, L. Fortuna, and M. Frasca, "Turing patterns in the simplest MCNN," Nonlinear Theory and Its Applications, IEICE, vol.10, no.04, pp.390-398, 2019.

[9] J. Gao, Y. M. Chen, "Finite-time and fixed-time synchronization for inertial memristive neural networks with time-varying delay and linear coupling," IAENG International Journal of Applied Mathematics, vol.52, no.3, pp.534-540, 2022.

[10] S. Belabssir and N. Sahlal, "Tensor product and linear error block codes," IAENG International Journal of Applied Mathematics, vol.51, no.2, pp.279-283, 2021.

[11] H. G. Othmer and L. E. Scriven, "Instability and dynamic pattern in cellular networks," Journal of Theoretical Biology. vol.32, no.3, pp.507-537, 1971.

[12] L. Goras and L. O. Chua, "Turing patterns in CNNs. II. Equations and behaviors," IEEE Transactions on Circuits and Systems I: Fundamental Theory and Applications, vol.42, no.10, pp. 612-626, 1995.

[13] Q. Ouyang and H. L. Swinney, "Transition from a uniform state to hexagonal and striped Turing patterns," Nature, vol.352, pp.610-612, 1991.

[14] L. C. Gu, S. H. Zhong, P. L. Gong, B. Wang, and H. Q. Wang, "Turing instabilities analysis and spatiotemporal patterns formation near a Hopf bifurcation," Engineering Letters, vol.28, no.4, pp.1031-1040, 2020.

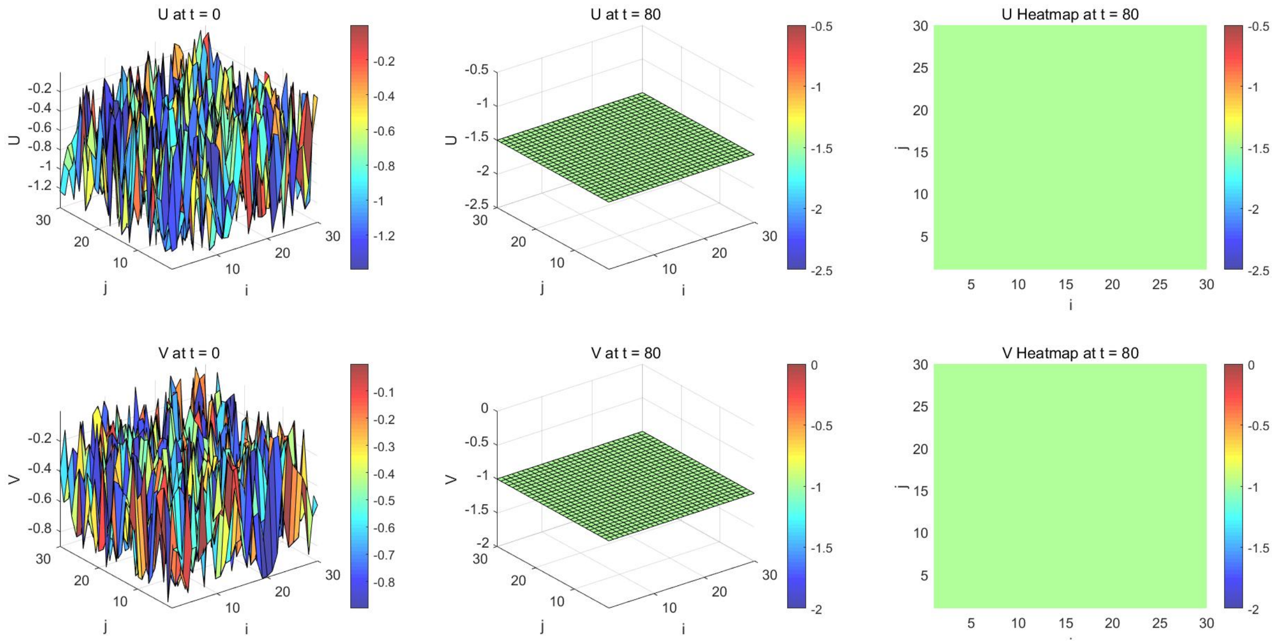

Fig. 2: Numerical Simulation for Group 1 in Table II with Randomized Initial Conditions.

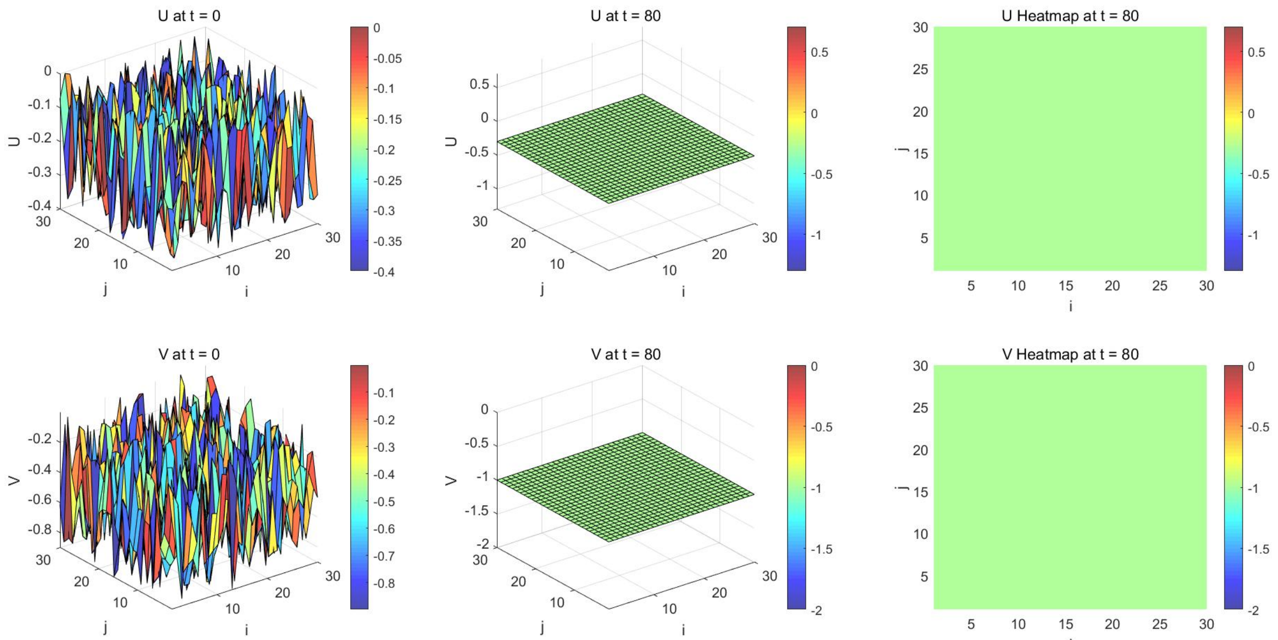

Fig. 3: Numerical Simulation for Group 2 in Table II with Randomized Initial Conditions.

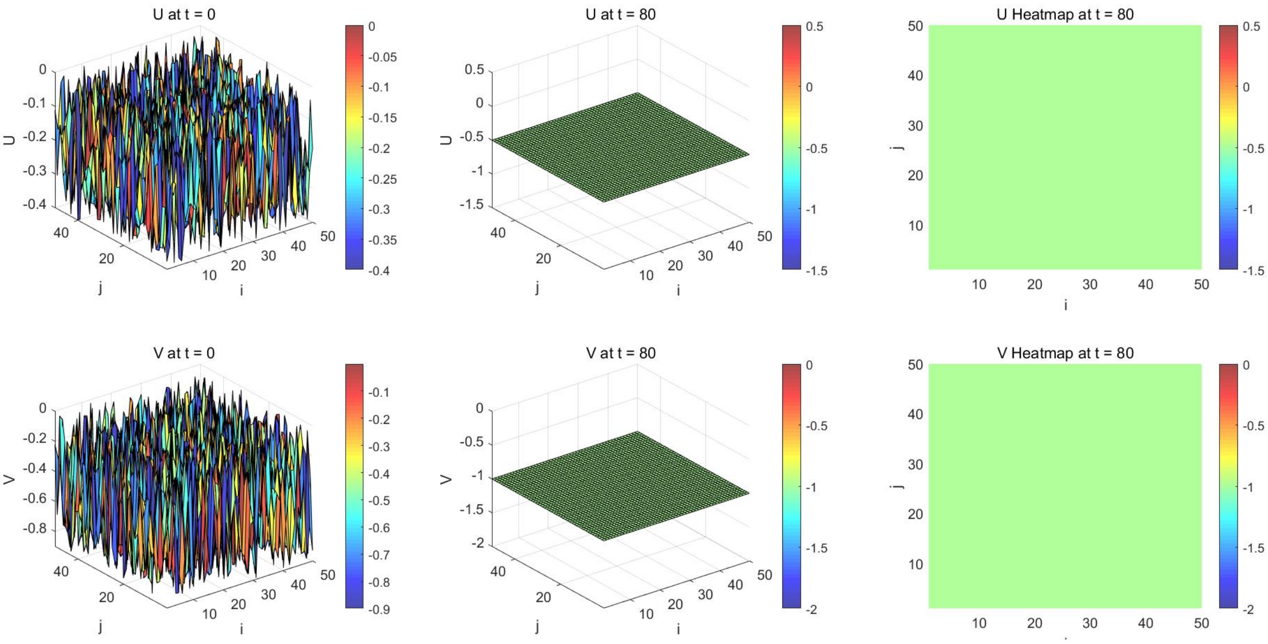

Fig. 4: Numerical Simulation for Group 3 in Table III with Randomized Initial Conditions.

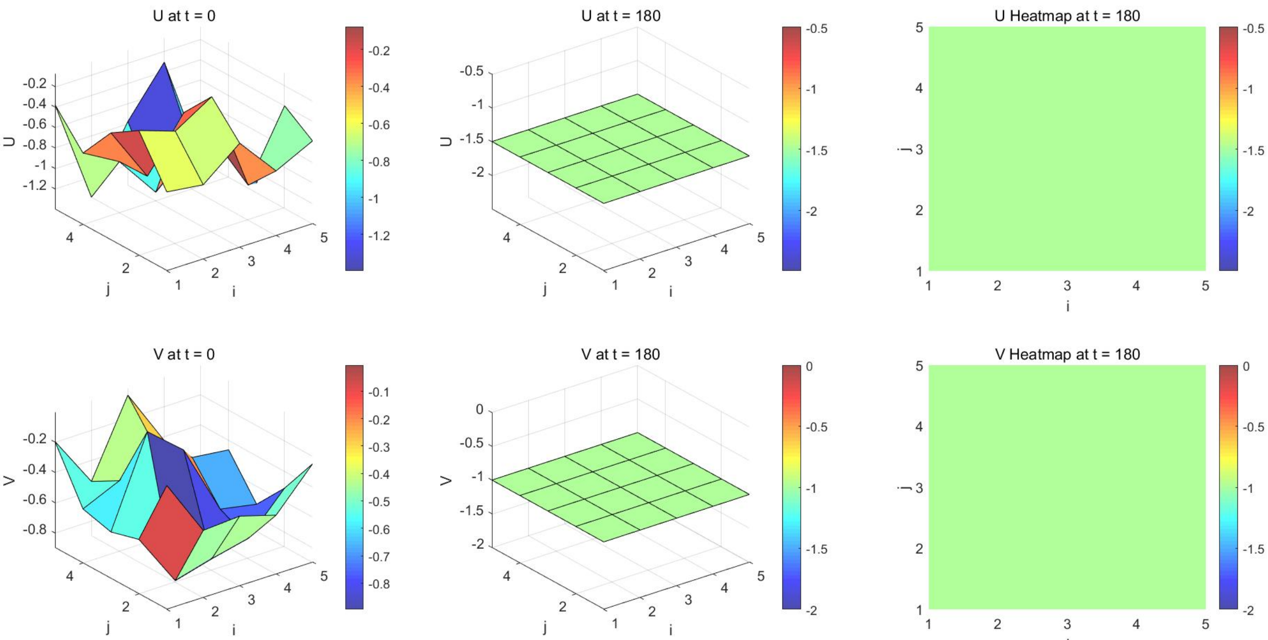

Fig. 5: Numerical Simulation for Group 4 in Table III with Randomized Initial Conditions.

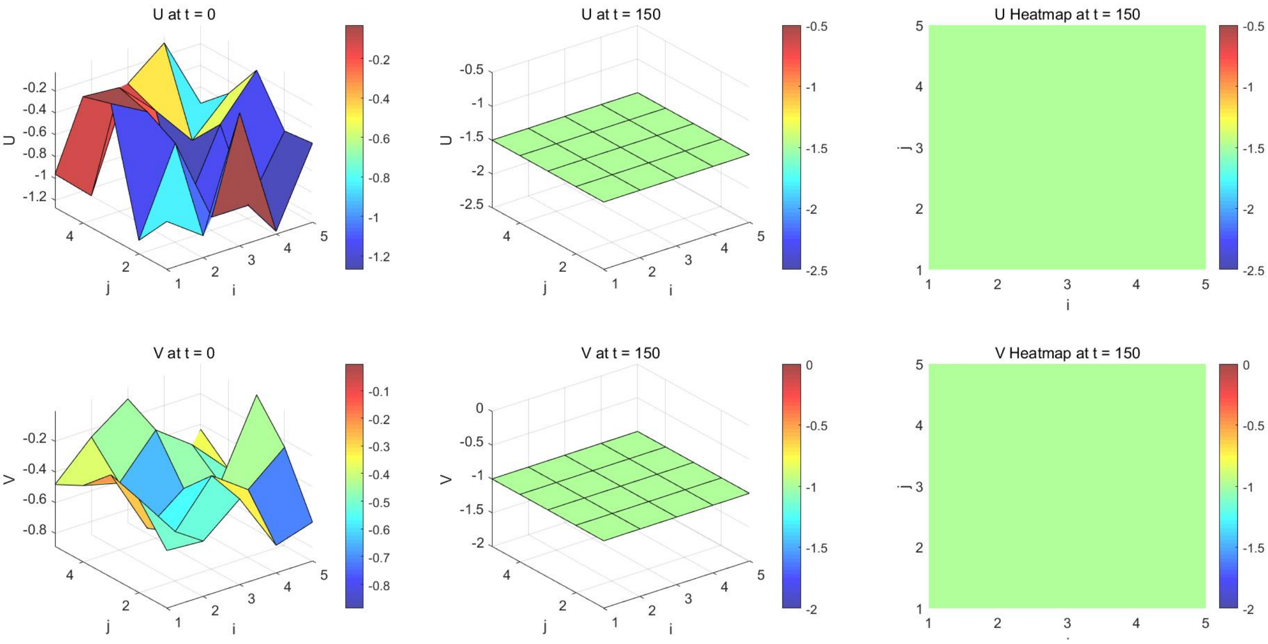

Fig. 6: Numerical Simulation for Group 5 in Table III with Randomized Initial Conditions.

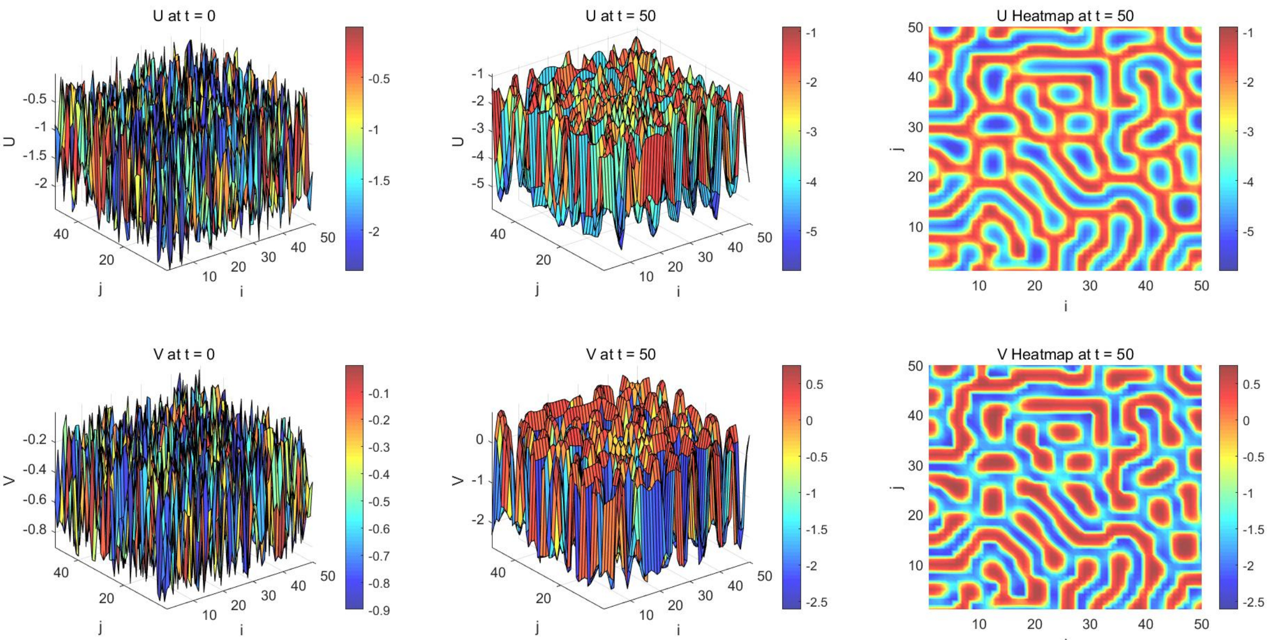

Fig. 7: Numerical Simulation for Group 6 in Table III with Randomized Initial Conditions.

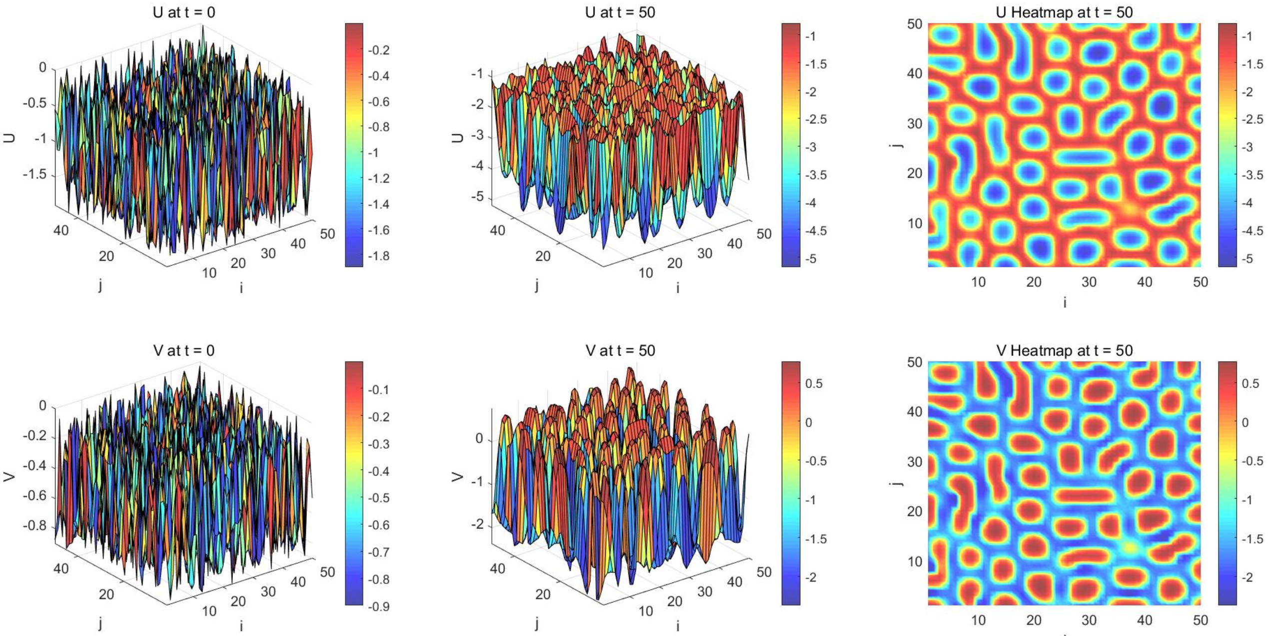

Fig. 8: Numerical Simulation for Group 7 in Table III with Randomized Initial Conditions.

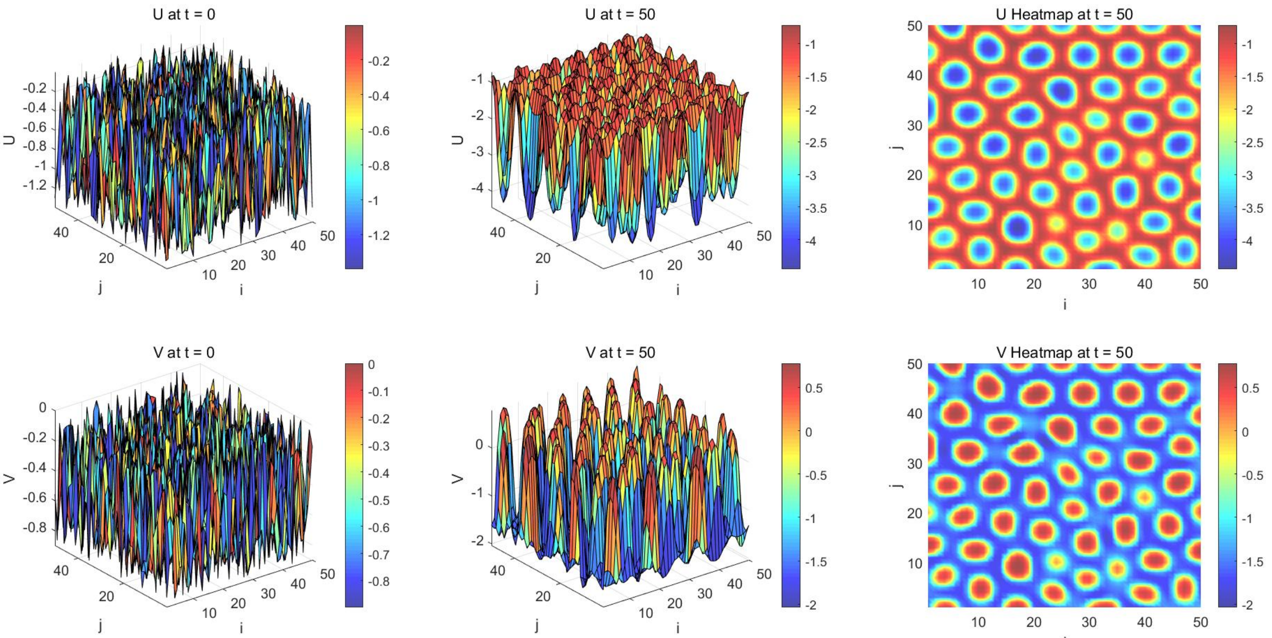

Fig. 9: Numerical Simulation for Group 8 in Table III with Randomized Initial Conditions.